Research Square

Preprints are preliminary reports that have not undergone peer review.
They should not be considered conclusive, used to inform clinical practice,
or referenced by the media as validated information.

Techno-economic and Optimization of Micro and Meso-porous Carbons for Sustainable CO_2 Capture

Marwa El Maghraby

marwa.maghraby93@gmail.com

Cairo University https://orcid.org/0009-0002-8918-9673

Ayat Osama Ghallab

Cairo University

Nabil M. Abdelmonem

Cairo University

Mahmoud M. Abdelnaby

King Fahd University of Petroleum and Minerals

Research Article

Keywords: Porous carbon, Carbon Capture, Chemical Activation, Pre-combustion, Techno-economics

Posted Date: November 13th, 2026

DOI: https://doi.org/10.21203/rs.3.rs-11707709/v1

License: This work is licensed under a Creative Commons Attribution 4.0 International License.
Read Full License

Additional Declarations: The authors declare no competing interests.

Techno-economic and Optimization of Micro and Meso-porous Carbons for Sustainable CO_2 Capture

Marwa A. El Maghraby *[a,b], Mahmoud M. Abdelnaby[c], A. O. Ghallab[a,d,e], Nabil M. Abdelmonem[a]

[a] Chemical Engineering Department, Faculty of Engineering, Cairo University, Giza 12613, Egypt

[b] Process Technology Division, Engineering for the Petroleum and Process Industries (ENPPI), Cairo 11768, Egypt

[c] Interdisciplinary Research Center for Hydrogen Technologies and Carbon Management (IRC-HTCM), King Fahd University of Petroleum & Minerals, Dhahran 31261, Saudi Arabia

[d] School of Energy and Environmental Engineering, Nile University, Giza 12588, Egypt

[e] Smart Engineering Systems Research Center (SESC), Nile University, Giza 12588, Egypt

Marwa A. El Maghraby, Marwa.maghraby93@gmail.com

Mahmoud M. Abdelnaby, mahmoudm@kfupm.edu.sa

Ayat O. Ghallab, ayatossama@cu.edu.eg

Nabil M. Abdelmonem, nabil.abdelmonem@yahoo.com

Corresponding Author: marwa.maghraby93@gmail.com

Abstract

Recently, carbon capture is very important to reduce the emissions of greenhouse gas. Conventional amine-based methods face limitations from high regeneration energy demand and toxic by-products, solid sorbent materials offer a promising alternative. In this study, cyanuric chloride-based polymer (CCP) and polymer-based porous carbon (PPC) are synthesized via solvothermal method and pyrolysis method; respectively. Potassium hydroxide (KOH) used as activating agent during pyrolysis process at activation temperatures ranging (600 – 900 °C) and KOH:polymer ratios varying from 1:1 to 4:1. The characterization of BET surface area shows that PPC synthesized at 900 °C and KOH:polymer ratio of 1:1 (PPC-900-1), gives the highest surface area of 1969 m^2/g compared to 60 m^2/g for CCP. The structure of all synthesized materials using PXRD and FTIR. Thermal stability is applied using TGA and the morphology analyzed using SEM and EDX. In terms of carbon capture application, PPC-900-1 provides moderate CO_2 uptake of 1.85 mmol/g at 298 K and 1 bar, and good selectivity of 2344 for 5% CO_2/H_2 mixture. These findings demonstrate that PPC-900-1 is a promising sorbent for CO_2 capture in the next-generation pre-combustion technology.

A techno-economic assessment showed that utility requirements (nitrogen and deionized water) dominate production costs ($1327/kg), far exceeding chemical ($45.92/kg) and energy inputs ($89/kg). The operating conditions contribute hugely on the production cost of the porous carbon materials. Although lower activation temperatures and higher KOH ratios reduced the overall cost per kilogram, synthesis at 900 °C and KOH ratio of 1:1 achieved the lowest cost per unit area ($0.74/$m^2$) while delivering the best material performance. This highlights the necessity of balancing cost efficiency with material performance to advance the scalability of porous carbon synthesized sorbent material used in pre-combustion carbon capture.

Keywords: Porous carbon; Carbon Capture; Chemical Activation; Pre-combustion; Techno-economics.

List of Abbreviations

Aluminum chloride	$AlCl_3$
Autothermal reforming	ATR
Brunauer-EmmettTeller	BET
Carbon element	C
Carbon dioxide	CO_2
Carbon monoxide	CO
Chlorine element	Cl
Cyanuric chloride	$C_3Cl_3N_3$
Cyanuric chloride-based polymer	CCP
Density functional theory	DFT
Dichloroethane	DCE
Direct air capture	DAC
Dual-Site Freundlich-Langmuir fit	DSFL
Energy Dispersive X-ray	EDX
Fourier Transform Infrared	FTIR
Grand canonical Monte Carlo simulations	GCMS
Hydrogen	H_2
Hydrochloric acid	HCl
Ideal adsorbed solution theory	IAST
Isosteric enthalpy of adsorption	ΔH_{ads}
Isosteric heat of adsorption	Qst
Metal-organic frameworks	MOFs
Methanol	CH_3OH/ MeOH
Oxygen element	O
Phosphoric acid	H_3PO_4
Polyacrylonitrile	PAN
Polyaniline	PANI
Polymer-based porous carbons	PPC

Polypyrrole	PPy
Pore size distributions	PSD
Potassium carbonate	K_2CO_3
Potassium element	K
Potassium hydroxide	KOH
Potassium oxide	K_2O
Powder X-ray diffraction	PXRD
Pressure swing adsorption	PSA
Response surface methodology	RSM
Scanning electron microscopy	SEM
Selectivity	S
Steam methane reforming processes	SMR
Thermogravimetric Analysis	TGA
Water	H_2O
Water-gas shift	WGS

1. Introduction

The worsening climate change crisis calls for immediate action to cut down greenhouse gases, especially carbon dioxide (CO_2), from industrial activities. The 2023 IPCC Report points out how dangerous the rise in emissions is and stresses the urgent need to take steps now to limit their impact (Segovia-Hernández et al., 2024). Likewise, the 2024 State of the Climate Report warns that fossil fuel emissions are at their highest ever, pushing global temperatures toward dangerous levels (Maka & Mehmood, 2024). Carbon can be captured using several methods, especially through pre-combustion, post-combustion, oxy-fuel combustion or directly from the atmosphere (DAC). The main technique of pre-combustion is applied to remove CO_2 from fuels before their burning (Mekonnin et al., 2025), while post-combustion capture soaks up CO_2 from the flue gases (Boretti, 2025). The fuel burns at oxy-fuel combustion under pure oxygen conditions leading to form flue gases contains water vapor and CO_2, making it easier to capture CO_2 (Taşğın et al., 2025). DAC, on the other hand, pulls CO_2 directly from the air using special chemical filters or sorbents (Jimenez-Lopez et al., 2025).

As global industrialization continues to rely heavily on fossil fuels for energy production, pre-combustion carbon capture technologies attracted attentions as a scalable solution which help in reducing CO_2 emissions from power plants, and other large-scale industrial systems (Vorokhta et al., 2025). The advancement of this technology depends on three key factors: how efficiently it operates, the thermodynamic benefits it offers, and how easily it can be integrated into existing industrial infrastructure. This method involves the separation of CO_2 from fuel gases before combustion, typically following gasification or reforming steps, and is particularly amenable to processes that produce hydrogen-rich fuels (Vogt & Weckhuysen, 2024). In this context, the development of high-performance solid sorbent materials is crucial, with porous carbon-derived polymers emerging as a leading candidate for implementation within the demanding environments of the oil and gas sector (X. Zhang et al., 2025). Porous carbon materials derived from polymers have emerged as exceptionally promising due to their unique combination of chemical affinity, tunable porosity, structural resilience, and regeneration capacity (Abdelnaby et al., 2023; Hui et al., 2025).

Refinery and petrochemical operations frequently involve hydrocarbon reforming, partial oxidation, or steam methane reforming processes (SMR) that generate syngas mixtures consist of hydrogen and carbon monoxide which converted into hydrogen and carbon dioxide through the reaction of water-gas shift reaction (Hu et al., 2025; Jankovic & Wilkinson, 2025; Makaryan & Sedov, 2023). Pre-combustion carbon capture seeks to extract CO_2 from this high pressure, hydrogen-rich gas stream before combustion or downstream usage (Baliga, 2024). This approach offers several intrinsic advantages: the elevated partial pressure of CO_2 simplifies the separation process (Mollahosseini et al., 2025); hydrogen, once purified, becomes blue hydrogen, which serves as a clean energy vector (van der Spek et al., 2022); and integration with existing process flows minimizes disruption to operations. However, the success of pre-combustion capture in refineries hinges on the availability of sorbents that can withstand harsh conditions-such as high temperatures, variable pressures, and the presence of multiple contaminants-while delivering high selectivity, capacity, and regeneration efficiency (Khosrowshahi et al., 2023). While traditional physical solvents like Selexol and Rectisol are widely used (Rana & Andino, 2025; Warrag & See, n.d.; Wilkes, 2023). The development of sorbent materials, particularly porous carbon-based materials, aims to address these limitations (R Maniarasu et al., 2021).

Porous carbons are characterized by their highly developed surface areas and various pore structures. The size of porous carbon is ranged from micropores (< 2 nm) to mesopores (2-50 nm) (Pinto et al., 2025; Zhigang Liu et al., 2025). This porous carbon provides numerous adsorption sites for gas molecules, making them ideal for carbon capture (Mishra et al., 2025). Porous carbon is an attractive platform for gas separation due to its chemical resilience, high surface area, tunable pore architecture, and environmental compatibility (Park et al., 2014). In its pure form, however, carbon lacks strong interactions with polar molecules like CO_2, especially in the presence of competing gases like H_2, CH_4, or N_2 (Kim & Kim, 2023; Min et al., 2023). To enhance its performance, nitrogen doping introduces basic sites into the carbon matrix, providing specific chemical functionalities that interact strongly with acidic gases (Choi et al., 2025; Shang et al., 2022). Nitrogen constituents in pyridinic-N, pyrrolic-N, and quaternary-N create localized electron-dense areas that favor electrostatic and hydrogen bonding interactions with CO_2 (Bandosz, 2021; Ma et al., 2025) . These groups increase selectivity, capacity and improve thermodynamic and absorption kinetics (Tachibana et al., 2022). Moreover, nitrogen doping enhances the wettability and surface polarity of carbon materials, which can be beneficial in

systems exposed to humidity or complex gas mixtures (Adeniji et al., 2025; L. Sun et al., 2014; Yu et al., 2023).

Synthesis of porous carbon used in carbon capture depends on the polymeric precursors with inherently high nitrogen content and structural versatility (Hryniewicka et al., 2025). Polymers such as polyacrylonitrile (PAN), polypyrrole (PPy), polyaniline (PANI), melamine-formaldehyde resins and cyanuric chloride-based polymer serve as ideal candidates due to their synthetic accessibility and ability to generate well-defined carbon structures upon pyrolysis (He et al., 2025; Tian et al., 2024). The synthesis approach for converting these polymers into porous carbons typically involves a carbonization stage followed by activation using activating agent such as; KOH, $ZnCl_2$, or H_3PO_4 to etch carbon matrix and generate porosity (Wabo & Klepel, 2021). Carbonization and activation stages transform the organic framework (polymer) into a graphitic or amorphous carbon network (porous carbon) while retaining or converting nitrogen groups into active adsorption sites (He et al., 2025; Vanreppelen et al., 2013). The process variables include heating rate, temperature, inert atmosphere, pyrolysis duration and type of activating agent play an important role in determining the final material's surface chemistry and textural properties (K. Wang et al., 2024). By modulating these variables, materials scientists can finely tune the pore size distribution (micropores for CO_2 entrapment, mesopores for diffusion), nitrogen species concentration, and overall architecture of the sorbents [42].

Cyanuric chloride-based porous carbon sorbents offer several advantages compared to traditional sorbents (Jadhav & Joshi, 2021). They are uniquely resilient options for pre-combustion carbon capture in oil and gas environments (Morales-Ospino et al., 2025; Sethia & Sayari, 2015). Their superior stability under chemically aggressive conditions, lower cost, and ease of regeneration (Sethia & Sayari, 2015). Their regeneration typically involves thermal desorption or pressure swing techniques, both of which can be integrated with the existing heat and pressure infrastructure within refineries, minimizing additional energy input (Abdelnaby et al., 2023). Additionally, their low heat of adsorption facilitates energy-efficient regeneration cycles, a key requirement for reducing operational costs in large-scale carbon capture facilities (Liu et al., 2025; H. Zeng et al., 2022).

This study aims to develop porous carbon materials exhibiting distinctive structural features and exceptionally high surface areas. Porous carbon materials are synthesized from nitrogen-rich

polymer precursor (cyanuric chloride), which is chemically activated using potassium hydroxide (KOH) at various weight ratios (ranging from 1-4) and subjected to different activation temperatures ranging from (600 – 900 °C). A techno-economic study has been conducted using Response Surface Methodology (RSM) to find the optimum conditions which provide optimum cost of chemical, utilities, energy, total cost and cost per area (Alakbari et al., 2023).

2. Experimental Work

2.1. Materials

Chemicals and reagents were utilized directly as obtained, with no purification or modification. The purity of each material are as follows; Benzene ≥ 99.7%, aluminum chloride 98%, hydrochloric acid 35% aqueous solution and potassium hydroxide pellets (ACS grade) ≥85%. The source of these materials is Sigma Aldrich. Cyanuric chloride $C_3Cl_3N_3$, 98%) is sourced from Alfa Aesar, while Loba Chemie is taken to be the source of 1,2-Dichloroethane (DCE). Double-distilled water is employed throughout the washing steps. Methanol (CH_3OH, 99.9%) is used during the final washing cycles to neutralize the samples. Monitoring PH by litmus paper which sourced from Sigma. High purity of nitrogen 99.99% is obtained from Air Liquide and also carbon dioxide with high purity.

2.2. Characterization

Pore structure is analyzed with N_2 adsorption isotherms using Quantachrome Autosorb iQ2 instrument. Brunauer-EmmettTeller (BET) method is utilized in surface area calculations. Pore size distributions (PSD) are analyzed using Density Functional Theory (DFT) fitting of N_2 adsorption data. The morphologies of the synthesized materials are measured using scanning electron microscopy (SEM) and JEOL JCM-7000 NeoScope, which is used to capture SEM images and embedded Energy Dispersive X-ray (EDX) Spectroscopy measurements. Powder X-ray diffraction (PXRD) of samples is analyzed using MiniFlex2 goniometer to measure crystallization and phase purity. The loss in mass of the material upon heating is obtained by Thermogravimetric Analysis (TGA). The molecular fingerprint of the sample has been tested by a Fourier Transform Infrared (FTIR) PerkinElmer 16 PC spectrometer. The recorded spectra are over 4000-500 cm^{-1} transmission mode. Carbon capture uptake analysis is performed using 2000-13, Quantachrome

instruments version 6.0, and the results have been taken from the software Quantachrome QuadraWin – Data Acquisition and Reduction for QuadraSorb SI.

2.3. Synthesis

This part is classified into two main parts including synthesis of both cyanuric chloride-based polymer (CCP) and polymer-based porous carbon (PPC).

2.3.1. Cyanuric chloride-based polymer (CCP) synthesis

Synthesis of CCP is performed following the previously reported method of hyper-crosslinked polymer (El Maghraby et al., 2026), except using the chemicals of $AlCl_3$, cyanuric chloride and benzene with quantities of 80 g, 27.66 g and 8.86 mL; respectively - instead of $FeCl_3$ and FDA - which mixed with dichloro ethane (DCE). These quantities are selected to maintain the specific stoichiometric ratios required for Friedel-Crafts polymerization, optimizing electrophilic aromatic substitution and controlling chain growth (Peter et al., 2024).

2.3.2. Polymer-based porous carbon (PPC) synthesis

Polymer-based porous carbon is synthesized by mixing 1 gram of the CCP polymer grounded with different ratios of KOH ranged 1 - 4. The resulting mixtures undergo pyrolysis at varies temperatures ranging from 600-900 °C for 2 hours under nitrogen conditions using horizontal tubular quartz reactor. After each experiment, the polymer-based porous carbon PPC is cooled down to room temperature. Porous carbons are neutralized with HCl (washing two times) to eliminate residuals of KOH followed by three rinses with deionized water and then washed with methanol multiple times until the pH of filtrate reached to 7. Synthesized PPC was then oven-dried at 80 °C overnight to ensure complete dryness. Synthesis conditions and methods are shown in Table 1.

Table 1

Synthesis conditions of CCP and PPC.

Samples	Polymer/Chemicals	Methodology	Temperature, °C	KOH: Polymer
CCP	Benzene + cyanuric chloride	Solvothermal (El Maghraby et al., 2026)	-	-
PPC-600-1	CCP	Pyrolysis	600	1:1
PPC-600-2			600	2:1
PPC -600-4			600	4:1
PPC-800-1			800	1:1
PPC-800-2			800	2:1
PPC-800-4			800	4:1
PPC-900-1			900	1:1
PPC-900-2			900	2:1
PPC-900-4			900	4:1

2.4. Techno-economic Analysis

The relationship between the following parameters: temperature, KOH ratio, and the cost response was obtained using RSM method using Design-Expert software (Alakbari et al., 2023)

The cost for synthesizing CCP and PPC is evaluated based on consumables, chemicals, solvents, and utilities. The consumables included $AlCl_3$, benzene, DCE, and cyanuric chloride, while methanol is considered among the solvents. Deionized water and nitrogen are used as utilities. In addition to hydrochloric acid which is used in washing. Chemicals prices are sourced from ECHEMI market prices of year 2025 (Echemi, 2025). The assumed unit costs are benzene ($807.35/metric ton), $AlCl_3$ ($0.10/kg), cyanuric acid ($3/kg), and KOH ($533.15/metric ton). Solvent prices of methanol and DCE are considered as $225.03/metric ton and $232.64/metric ton; respectively. Hydrochloric acid price is taken as $6.92/metric ton.

Utility costs are estimated using market references. The price of deionized water of $1.95/$m^3$ is considered as per Saudi Marafiq of year 2025 (Marafiq Saudi Arabia, 2025), while nitrogen is

valued at $0.10 per cubic meter as per market analysis of year 2025 (Imarcgroup, 2025). The cost of oil bath is assumed to be $4000 per metric ton as per ECHEMI (Echemi, 2025). Electrical costs are calculated on the basis of actual power requirements. Local factor of α is used to adjust both the capacity of synthesized material and energy consumption whereas the laboratory scale operates above this capacity. This factor represents the ratio of maximum equipment capacity to the actual required capacity, as reported (Abdalla et al., 2025; El Maghraby et al., 2026). Furthermore, the electricity cost was taken at $0.053/kWh, corresponding to the 2025 electricity rates for Saudi Arabia documented by Global Petrol Prices (Saudi Electricity Global Petrol, 2025)

The total synthesis cost of CCP and PPC is calculated by combining the expenses of chemicals, utilities, and energy consumption (El Maghraby et al., 2026). To obtain efficient comparison, the total cost was calculated per kg of sorbent as reported (Abdalla et al., 2025; El Maghraby et al., 2026). These values provide the foundation for assessing the economic inputs of the synthesized materials and allowing assessment of their cost-effectiveness.

3. Results and discussion

3.1. Porosity and Textural Structure

Cyanuric chloride-based polymer (CCP) and polymer-based porous carbon (PPC) materials are synthesized as previously mentioned in Table 1 using solvothermal method for CCP and pyrolysis method for PPC synthesis.

CCP and PPC characterization are illustrated in Table 2 including BET surface area, micropore surface area, mesopore surface area, total pore volume and micropore volume. It is clear that, PPC porous carbon synthesized at 900 °C using ratio 1:1 gives largest surface area of 1969 m^2/g while CCP recorded lower value of 60 m^2/g. This means that Potassium hydroxide (KOH), under elevated temperatures, undergoes a series of redox reactions with carbon, yielding components such as potassium carbonate, potassium oxide and metallic potassium, alongside gaseous byproducts including hydrogen (H_2), water vapor, carbon dioxide and carbon monoxide (Li et al., 2013; Ma et al., 2020). The usage of chemical agents in the activation process leading to etching which then develop the pores (Li et al., 2013; Ma et al., 2020).

Table 2 shows that activation temperature has a positive impact on increasing BET surface area. As temperature increases, the surface area increases directly at constant KOH: polymer ratio 1:1 which is consistent with findings from previous research (J. Chen et al., 2022; Kunjumon et al., 2025a). Notably, BET surface area of the precursor CCP (60 m^2/g) increased significantly to 98 m^2/g, 1388 m^2/g and 1969 m^2/g for the respective materials at activation temperature 600, 800 and 900 °C, respectively. This means that BET surface area has been enhanced via activation temperature. In addition, the total pore volume of CCP (0.046 cm^3/g) is increased to 0.073, 0.66, 1.331 cm^3/g for PPC using temp 600, 800 and 900 °C, respectively at constant ratio. Also, micropore volume of CCP 0.026 cm^3/g is increased to 0.027, 0.518 and 0.772 cm^3/g for PPC using temp 600,800 and 900 °C, respectively. It is clear that activation temperature at 900 °C pronounced microporous characteristics, playing a critical role in its superior adsorption performance.

As shown in Fig. 1, it is clear that the most pore size distribution of CCP and PPC fall below 2 nm with small fraction fall in the range 4-6 nm. These findings confirm the existence of micropores and mesopores, as proved in Table 2. The nitrogen isotherms in Fig. 1 indicate that CCP and porous carbon materials have the same pattern, which exhibits reversible type I(a) behavior, characteristic of microporous materials with limited external surface area (typically < ~2 nm).

Table 2

Summary of the porosity properties of the synthesized materials.

Material	BET Surface Area (m^2/g)	Micropore Surface Area (m^2/g)	Mesopore Surface Area (m^2/g)	Total Pore Volume (cm^3/g)	Micropore Volume (cm^3/g)	DFT Median Pore Radius (Å)
CCP	60	44	16	0.046	0.026	15.6
PPC-600-1	98	59	39	0.073	0.027	14.8
PPC-600-2	261	197	64	0.17	0.089	13.08
PPC-600-4	355	300	55	0.198	0.135	11.17
PPC-800-1	1388	1262	126	0.660	0.518	9.5
PPC-800-2	851	788	63	0.404	0.318	9.5
PPC-800-4	801	693	108	0.368	0.238	9.2
PPC-900-1	1969	1421	548	1.331	0.772	13.5

PPC-900-2	1198	1054	144	0.655	0.495	11.0
PPC-900-4	1143	1002	141	0.642	0.505	11.2

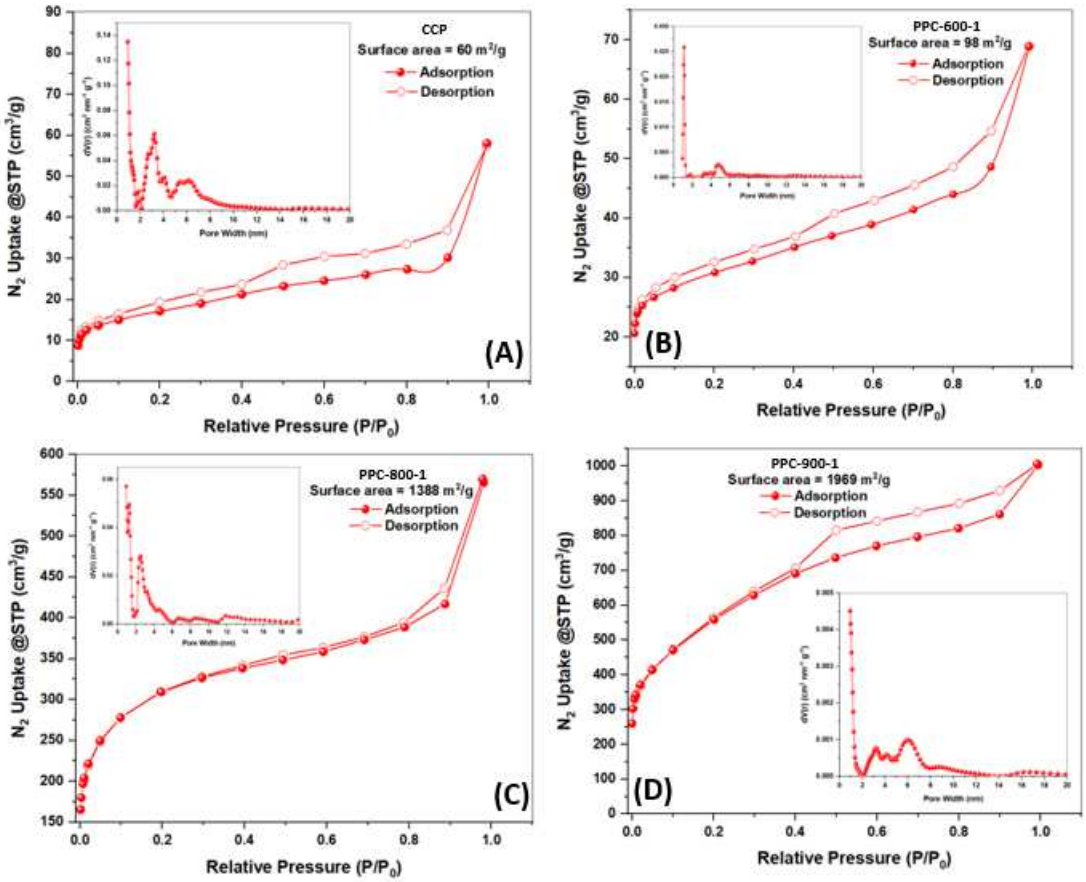


Fig. 1. Isotherm and pore size distribution for; (A) synthesized polymer CCP, (B) porous carbon at 600 °C and KOH:Polymer 1:1, (C) porous carbon at 800 °C and KOH:Polymer 1:1, (D) porous carbon at 900 °C and KOH:Polymer 1:1.

Table 3 shows the effect of activation temperature using different KOH ratio on BET surface area as reported in the literature compared to this work. At KOH ratios 1 and 2, moderate surface areas are observed. The synthesized material BET surface area of PPC at temperature 900 °C and KOH ratio 1:1 (PPC-900-1) of 1969 m²/g in this study compared to 1700 m²/g at same conditions

obtained in previous work (Lee et al., 2017), PPC-900-1 is considered the largest surface area reported for porous carbons.

Table 3

BET surface area for the porous carbons in the literature via KOH activation.

Temperature, °C	KOH Ratio	BET Surface Area (m^2/g)	Ref
900	4	1668	(Yang et al., 2014)
500	4	749	(Yang et al., 2014)
800	4	1900	(Lee et al., 2017)
600	2	1884.2	(P. Zhang et al., 2019)
600	2	1700	(Sevilla et al., 2011)
550	4	882	(Li et al., 2016)
600	1	797	(Li et al., 2016)
600	2	1923	(Li et al., 2016)
600	4	1893	(Li et al., 2016)
650	1	1023	(Li et al., 2016)
650	2	1707	(Li et al., 2016)
650	4	1411	(Li et al., 2016)
900	1	1700	(Lee et al., 2017)
900	1	1969	This work

3.2. Structure Characterization

All samples are subjected to powder X-ray (PXRD) analysis. In comparison of CCP and PPC at different conditions, it is clear that CCP displays abroad hump at $2\theta \approx 25°$, reflected to the (002) which proof the material of amorphous carbon (X. Chen et al., 2024; Kunjumon et al., 2025a; Ma et al., 2020). As illustrated in Fig. 2, the absence of sharp diffraction peaks further confirms its non-crystalline nature.

On the other hand, synthesized materials at 600, 800, 900°C at 1:1 provide the same pattern of original CCP. The resulting porous carbon synthesized at 900 °C showed PXRD patterns with same structural characteristics of the original CCP, with an additional broad peak appearing at $2\theta \approx 44°$, consistent with previous literature [59].

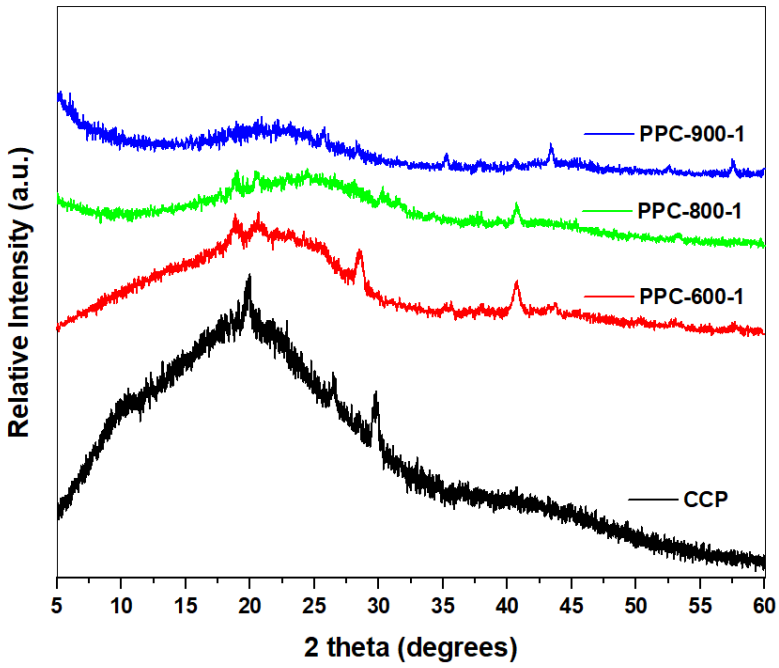


Fig. 2. PXRD for CCP and PPC at different temperatures.

As illustrated in Fig. 3. Existence of aliphatic and aromatic stretching supports their carbonaceous nature. Fig. 3 shows that the synthesized porous carbon at 900 °C and ratio 1:1 (PPC-900-1) displays a distinct N-H stretching band at 3425 cm^{-1} (Li et al., 2016), while weaker bands near 2920 cm^{-1} and 2850 cm^{-1} are also evident (Fan et al., 2013; Li et al., 2016). A prominent peak at 1620 cm^{-1} corresponds to C=C stretching in aromatic rings (Li et al., 2016; Sevilla et al., 2011), accompanied by a shoulder near 1700 cm^{-1} likely attributable to C=O stretching vibrations (Li et al., 2016; Sevilla et al., 2011). Broad absorptions spanning 1370-1250 cm^{-1} are associated with C-O-H bending and C-N stretching modes (Li et al., 2016; Sevilla et al., 2011; Y.-B. Sun et al., 2014). Additionally, weak bands within the 900-650 cm^{-1} region are assigned to N-H or C-H out-of-plane deformation vibrations (Fan et al., 2013; Li et al., 2016; Zelenak et al., 2008). Therefore, these findings mean that N-H and C-N groups are present in PPC-900-1. On the other hand, CCP,

PPC-600-1 and PPC-800-1 show bands of absorption at 3600 and 3700 cm^{-1} (R. Zeng et al., 2021). The presence of C-H stretching shown at 1083 and 885 cm^{-1} (J. Chen et al., 2022). Furthermore, aromatic stretching appeared at 2915 and 3000 cm^{-1} (J. Chen et al., 2022).

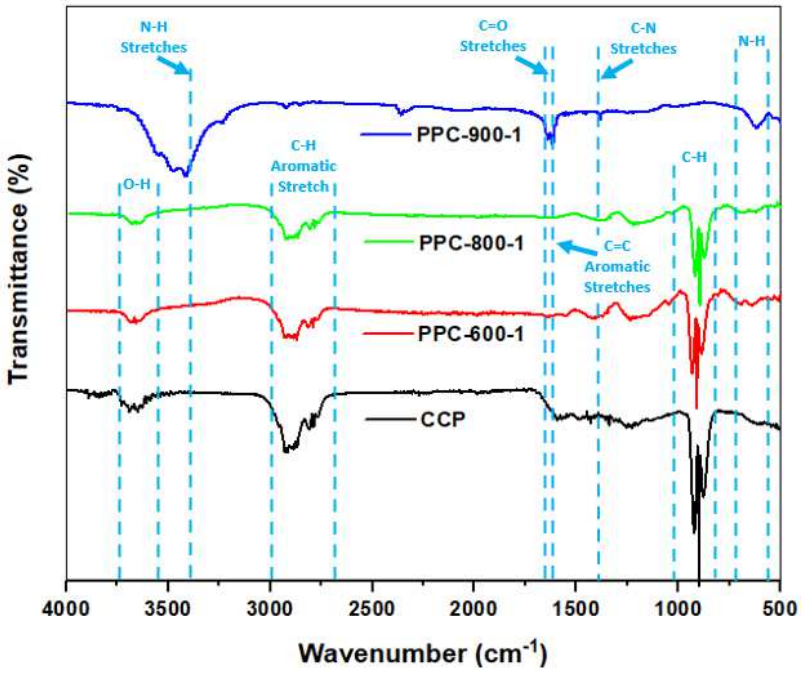


Fig. 3. FTIR for CCP and PPC at different temperatures.

Thermal stability of porous carbon is highly affected by the presence of micro and mesopores. Prior research (Van Der Voort et al., 2002) indicates that micropores are more resistant to high-temperature activation than mesopores. Therefore, porous carbons with higher thermal stability are preferable, leading to development of reliable and durable porous carbon structures. On the other hand, porous carbons with lower thermal stability tend to generate mesoporous frameworks that are less resistant to heat. Fig. 4 shows the thermogravimetric analysis (TGA) of synthesized CCP and PPC at different temperatures using KOH:polymer ratio 1:1. It is clear that synthesized PPC at high temperatures (800, 900°C) have high thermal stability than that synthesized at low temperature 600 °C. The weight loss of both PPC-800 and PPC-900 begin at high temperatures above 500 °C compared to CCP and PPC-600 which have weight loss at below 350 °C. Thus, PPC-900-1 has good thermal stability with minimal residual mass beyond 500 °C.

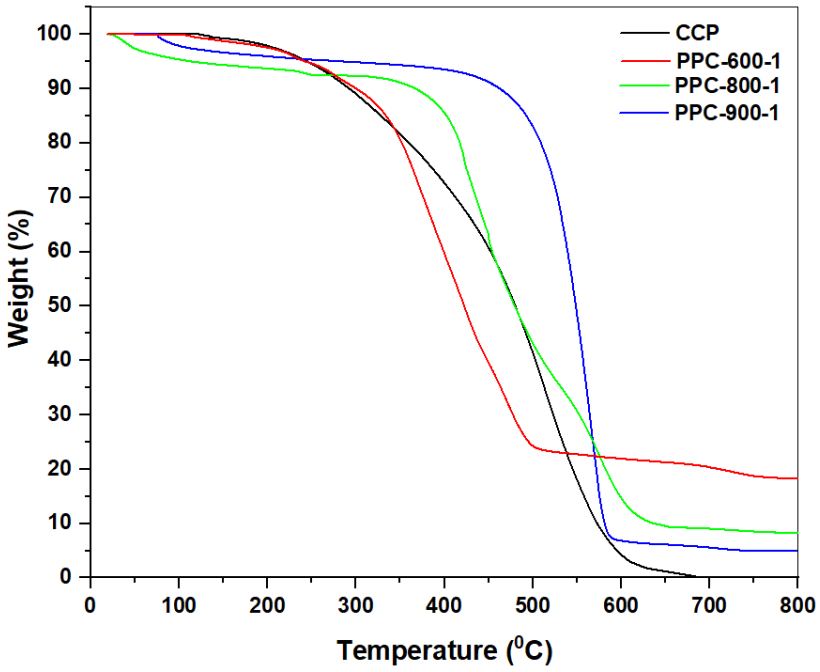
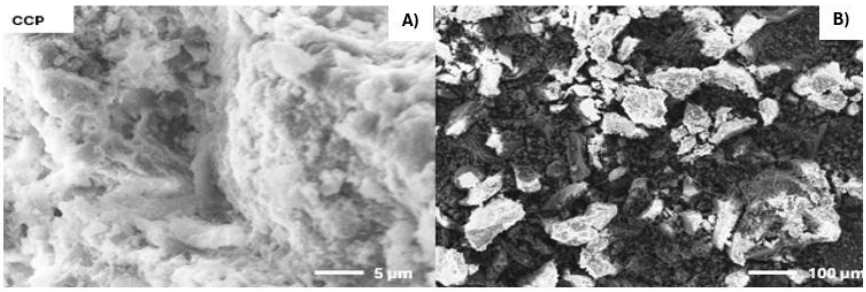


Fig. 4. TGA for CCP and PPC at different temperatures.

The morphology of the materials is characterized by using SEM (JEOL JCM-7000) to evaluate phase purity and structural uniformity. As illustrated in Fig. 5, the precursor exhibits an amorphous architecture composed of nanostructured particle clusters (X. Chen et al., 2024; Kunjumon et al., 2025a). Porous carbon (PPC-900-1) displays a densely packed porous surface, as shown in Fig. 6. Furthermore, PPC-900-1 exhibits an amorphous structure with pores of different sizes distributed across its surface (Vorokhta et al., 2025). The EDX spectrum of CCP confirmed the existence of oxygen, carbon and chlorine, originating from its synthesis process. In the EDX profile of PPC-900-1, trace amounts of potassium (K) were detected, likely introduced during the chemical activation with potassium hydroxide.



Element	Line	Mass%	Atom%
C	K	65.71±0.60	72.83±0.66
O	K	31.31±1.06	26.05±0.88
Cl	K	2.99±0.16	1.12±0.06
Total		100.00	100.00
Spc_001			Fitting ratio 0.3067

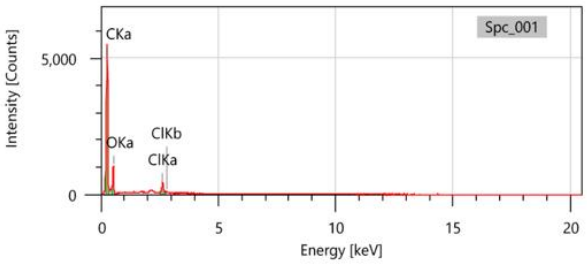
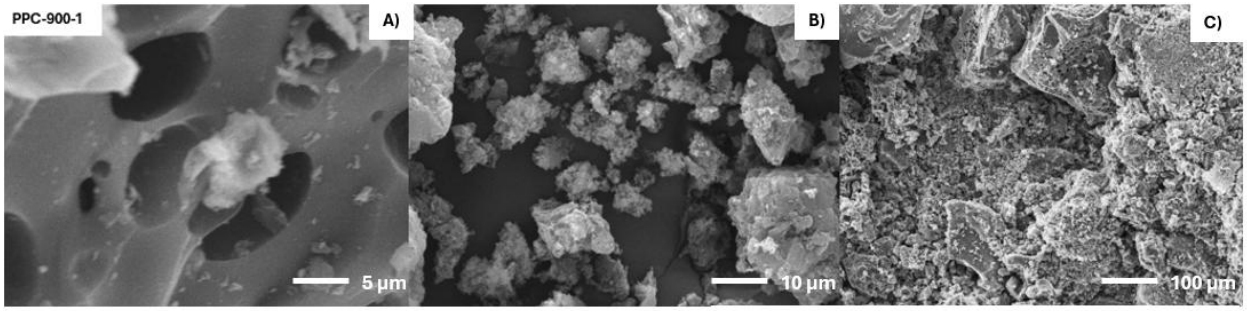


Fig. 5. SEM and EDX for CCP at, (A) low magnification of 5 µm and (B) high magnification of 100 µm.



Element	Line	Mass%	Atom%
C	K	56.28±0.56	68.87±0.68
O	K	24.74±0.94	22.73±0.86
Al	K	7.09±0.22	3.86±0.12
S	K	0.66±0.07	0.30±0.03
Cl	K	0.39±0.06	0.16±0.02
K	K	10.84±0.33	4.07±0.12
Total		100.00	100.00
Spc_001			Fitting ratio 0.2303

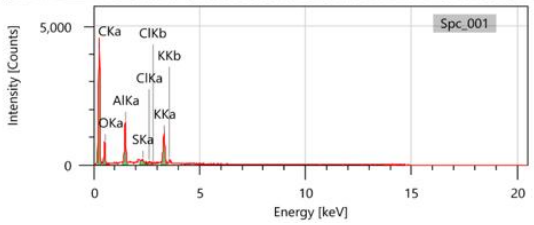


Fig. 6. SEM and EDX for porous carbon at temperature 900 and KOH:polymer ratio 1:1 at, (A) low magnification of 5 µm, (B) moderate magnification of 10 µm and (C) high magnification of 100 µm.

3.3. CO_2 Capture and Measurements

3.3.1. CO_2 adsorption

The isotherm of CO_2 adsorption for porous carbon, obtained through volumetric analysis at 273 K, 298 K, and a pressure of 1.13 bar, are presented in Fig. 7. The adsorption performance is improved at high temperature, high degree of microporosity and the presence of nitrogen groups (Alabadi et al., 2016). Synthesized material PPC-900-1 is selected in the analysis of CO_2 capture due to its high BET surface area.

Fig. 7 presents the CO_2 adsorption isotherms of porous carbon PPC-900-1 synthesized through soft chemical activation. The mildly activated carbon PPC-900-1 exhibits CO_2 uptake capacities, ranging from 2.44 to 51.86 cm^3/g (0.11 to 2.31 mmol/g) at 273 K and 0.4 to 41.44 cm^3/g (0.02 to 1.85 mmol/g) at 298 K, as stated in Fig. 7. PPC-900-1 is considered the highest proven CO_2 uptake among the studies at a temperature of 900 °C. These results highlight the effectiveness of systematically optimizing parameters such as specific surface area and adjustable pore size to enhance CO_2 capture performance in porous carbon materials (Alabadi et al., 2016; Li et al., 2016). The synthesized PPC-900-1 outperforms the CO_2 capture close to the reported materials in the literature. Examples include NMC-800 (2.5 mmol/g) (Alabadi et al., 2016; Zhou et al., 2015) , PP1-2 (1.5 mmol/g) (Alabadi et al., 2016; Xu et al., 2015), AC (1.5 mmol/g) (Alabadi et al., 2016; Cong et al., 2015), and CS3-A6 (2.6 mmol/g) (Alabadi et al., 2016; Mahurin et al., 2014). It also competes with top-tier sorbents such as NPC-650 (2.4 mmol/g) (Alabadi et al., 2016; J. Wang et al., 2013) and MR-1-500 (2.2 mmol/g) (Alabadi et al., 2016; Cong et al., 2015). Given these results, PPC-900-1 holds strong potential for industrial CO_2 capture applications, particularly in the pre-combustion technique. It is noteworthy that the adsorption and desorption branches of the isotherms are perfectly superimposed, displaying no hysteresis loops as shown in Fig. 7. This indicates that the sorbents can be fully regenerated under vacuum conditions without the need for heat input. It is widely noted that a microporous structure combined with the Cyanuric chloride-based polymer precursor (CCP) significantly enhances CO_2 capture and separation performance, particularly in the presence of ultra-micropores (<1 nm) and nitrogen (N) heteroatoms (Deng et al., 2014; Xing et al., 2012; P. Zhang et al., 2019). Ultra-micropores offers space for gas molecules and traps them through Van der Waals interactions. Surface polarity and basicity is increased by N

heteroatoms and hence weak chemical interaction forces between CO_2 molecules and sorbent surface is promoted (Suo et al., 2017) .

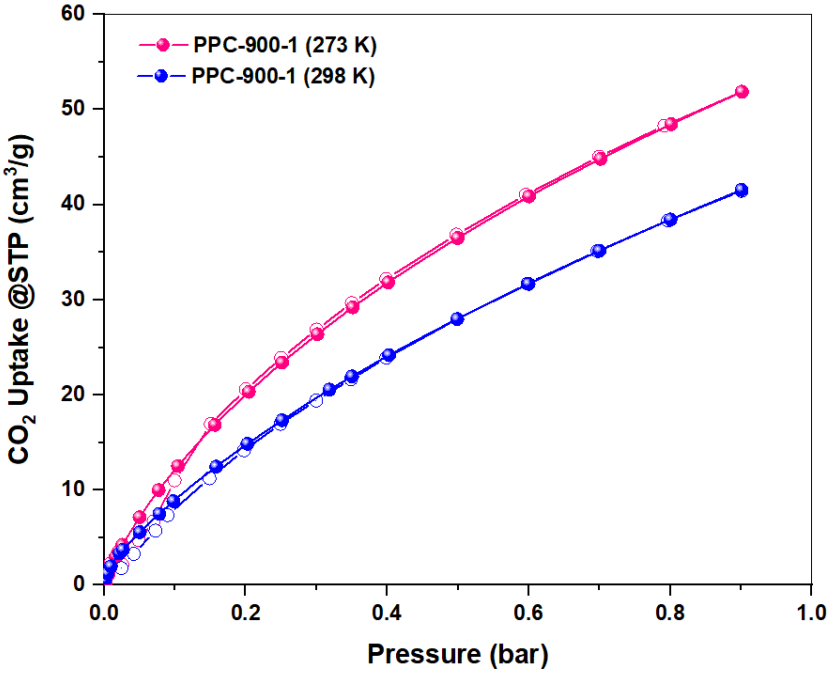


Fig. 7. CO_2 Adsorption-desorption isotherms for porous carbons PPC-900-1 at 298 K and 273 K at atmospheric pressure.

3.3.2. CO_2 isosteric heat of adsorption (Qst)

Isosteric heat of adsorption represents the heat amount required to attach or detach the adsorption molecule from the surface of solid sorbent (Nuhnen & Janiak, 2020). To effectively separate two components from a gaseous mixture, each component must exhibit different interaction energies with the sorbent surface-assuming equal accessibility to that surface, so that one is more readily adsorbed than the other. Amount of adsorption adsorbed is affected by temperature, relative pressure and strength of sorbent interaction. It is worth noting that the terms "heat of adsorption," "isosteric heat of adsorption" (Q_{st}), and "isosteric enthalpy of adsorption" (ΔH_{ads}) are often used interchangeably to describe this interaction energy (Nuhnen & Janiak, 2020). In general, materials intended for adsorption applications must fulfill several criteria, including high selectivity, low energy requirements for regeneration, and substantial working capacity(Keskin et al., 2010). Thus,

the enthalpy of adsorption plays a crucial role in evaluating adsorption performance and serves as a key indicator for understanding the interactions between the adsorbate and the sorbent.

Methods for determining the enthalpy of adsorption (ΔH_{ads}) fall into two main categories: experimental calculations and molecular simulations. Simulated values are typically derived from isotherms generated via grand canonical Monte Carlo simulations (GCMS) and computed the ensemble fluctuation method (Du et al., 2020). Experimental approaches, in contrast, include both direct and indirect techniques. Calorimetric volume system is used in direct method to evaluate the heat obtained during adsorption. system to measure the heat released during adsorption, but due to its complexity and high cost, it is rarely employed [84,85]. The indirect method-by far the most commonly used-involves analyzing adsorption isotherms, where the adsorbate– sorbent interaction energy is inferred from isotherms measured at two closely spaced temperatures (T_1 and T_2), typically with a temperature difference (ΔT) of 10-20 K (Nuhnen & Janiak, 2020). Therefore, CO_2 Q_{st} has been calculated considering temperatures at 273 K and 298 K.

In this study, the Clausius–Clapeyron approach is used via Dual-Site Freundlich-Langmuir fit (DSFL). The DSFL fitting approach demonstrates higher reliability, particularly at low adsorbate uptakes under low-pressure conditions. This observation aligns well with existing literature, which consistently reports that DSFL offers superior fitting accuracy compared to the Freundlich-Langmuir (FL) method and other modeling approaches (Avelar Dutra et al., 2017; Caldwell et al., 2015; Nuhnen & Janiak, 2020). Notably, the dual-site framework proves especially valuable for evaluating isosteric enthalpies across a wide loading range, beginning from near-zero adsorption levels. The calculated isosteric heat of adsorption (Q_{st}) for PPC-900-1 is recorded at 17.8 kJ/mol at zero CO_2 adsorption loading, as shown in Fig. 8a. PPC-900-1 has the largest mesoporous surface area of 548 m^2/g, as shown in Table 2. This indicates that as mesoporosity increases, CO_2 has a stronger affinity with the material at low pressure, leading to higher Q_{st}. The Q_{st} values remain within the physisorption range of < 35 kJ/mol, which possesses easier regeneration of the sorbent (Thommes et al., 2015).

To assess the regeneration ability and stability of PPC-900-1, three consecutive adsorption–desorption cycles were performed using the Autosorb apparatus, as illustrated in Fig. 8b. During each cycle, a continuous CO_2 stream was passed through the adsorption chamber at 273 K.

Subsequently, the sample was regenerated under the same conditions. The negligible decline in CO_2 uptake across cycles confirms the material's stability and potential for industrial reuse.

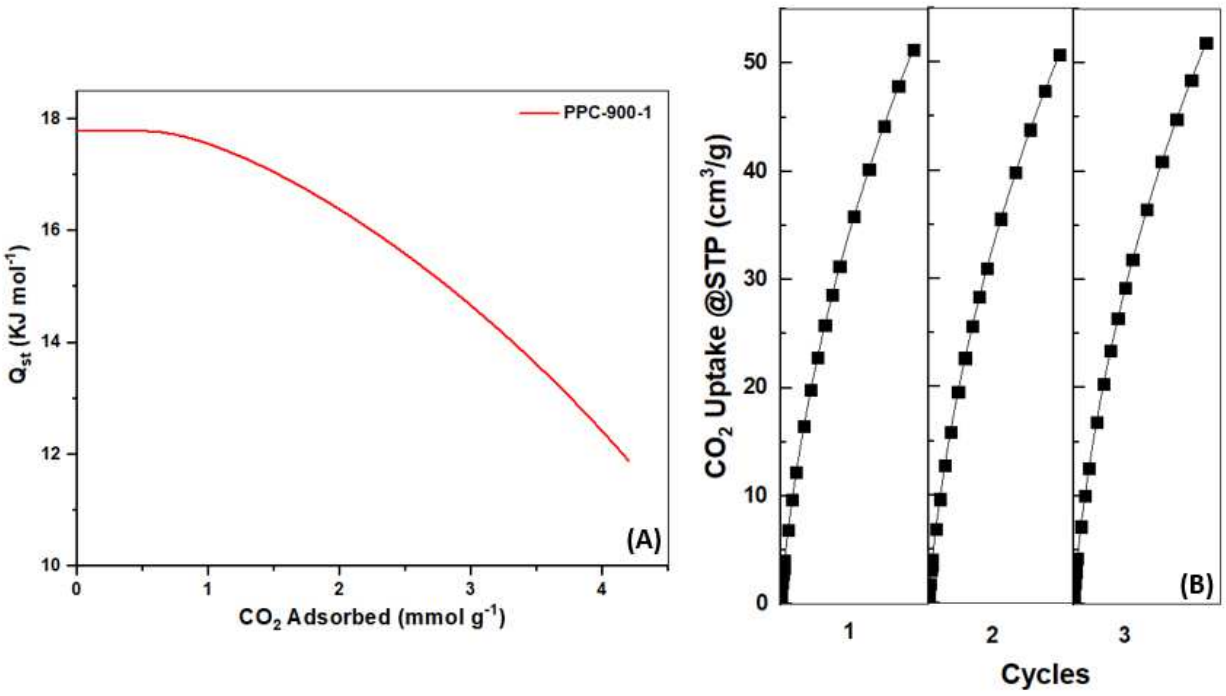


Fig. 8. (A) CO_2 Isosteric heat of adsorption for PPC-900-1 calculated at 273 K and 298 K using the Clausius-Clapeyron equation. (B) Recycling performance of PPC-900-1 at 273 K and 0-1.0 bar.

3.3.3. CO_2 selectivity

The unique CO_2 uptake exhibited by the synthesized micro and mesoporous carbon PPC-900-1 indicates their potential suitability for separating CO_2 from syngas, which possesses high H_2 content. Syngas, produced from steam methane reforming (SMR) and autothermal reforming (ATR), primarily contains H_2 and CO_2, along with minor concentrations of impurities such as CO, CH_4, N_2, and argon. After passing through the water-gas shift (WGS) reactor, these streams are delivered at elevated pressure and subsequently cooled to room temperature before passing to the pressure swing adsorption (PSA) unit for the purification of hydrogen (Streb et al., 2019). Generally, stream after WGS contains 71-75% H_2, 15-20% CO_2, and approximately 5% other components (Cox & Mokaya, 2017). To assess CO_2 selectivity, the high-pressure adsorption behavior of CO_2 and H_2 for PPC-900-1 was evaluated. Selectivity was further analyzed for PPC-900-1 using CO_2/H_2 mixtures with compositions closely resembling typical syngas. Uptake values for CO_2 and H_2 at 1 bar and 25 °C reached 44 cm³/g and 0.65 cm³/g in synthesized material PPC-

900-1, as shown in Fig. 9a,9b. CO_2 uptake values are much higher than those of H_2 uptake on the material, resulting preference for CO_2.

As illustrated in Fig. 9c, equilibrium CO_2/H_2 adsorption ratios were plotted against pressure for PPC-900-1. At low pressure, the material exhibited a high ratio of 117. At elevated pressures, the CO_2/H_2 ratio for PPC-900-1 decreased substantially to 67.7 at 1 bar, CO_2 uptake and H_2 uptake reached 44 cm^3/g and 0.65 cm^3/g; respectively. These results demonstrate that the material PPC-900-1 offers superior performance for CO_2 separation and H_2 purification at 1 bar and 25 °C. CO_2 selectivity can also be evaluated using syngas stream composed of H_2/CO_2 mixture with ratio of 80:20 (Cox & Mokaya, 2017). This ratio mirrors typical syngas compositions, which generally consist of 71-75% hydrogen and 15-20% carbon dioxide, making it a realistic basis for estimating CO_2 preference. The assessment relies on the ideal adsorbed solution theory (IAST) model which was used to determine relative adsorption in binary gas mixtures. According to IAST, the selectivity (S) for CO_2 is calculated same as previously reported (Cox & Mokaya, 2017; Kunjumon et al., 2025b). Fig. 9d presents the IAST-based CO_2 selectivity profiles across varying pressures with CO_2/H_2 range 5-20%. PPC-900-1 (5% CO_2) shows the highest selectivity of 2344 compared with PPC-900-1 at CO_2/H_2 10%, 15% and 20% of 1170, 781, and 586, respectively. A pattern is observed that shows a decrease in CO_2 selectivity as CO_2/H_2 increases. This indicates that the material is very selective to CO_2 at low CO_2/H_2. Yet, as pressure rises, the selectivity of PPC-900-1 decreases. It was observed that as pressure increases, CO_2 uptake increases in Fig. 9a; however, CO_2 selectivity decreases in Fig. 9d. This shows that at low pressure, CO_2 maintains stronger interactions than other gases due to its quadrupole moment- making it more selectively adsorbed. On the other hand, CO_2 uptake depends heavily on partial pressure. Lower pressure means fewer CO_2 molecules are available to be adsorbed. Even if the system prefers CO_2 over other gases, the driving force for mass transfer is weaker. In this case, CO_2 is more “preferred,” but there’s just not enough of it to grab onto the material. PPC-900-1 porous carbon performance enhancement is contributed to its substantial mesopore volume and high surface area, which provide a strong affinity for CO_2 capture in pre-combustion applications.

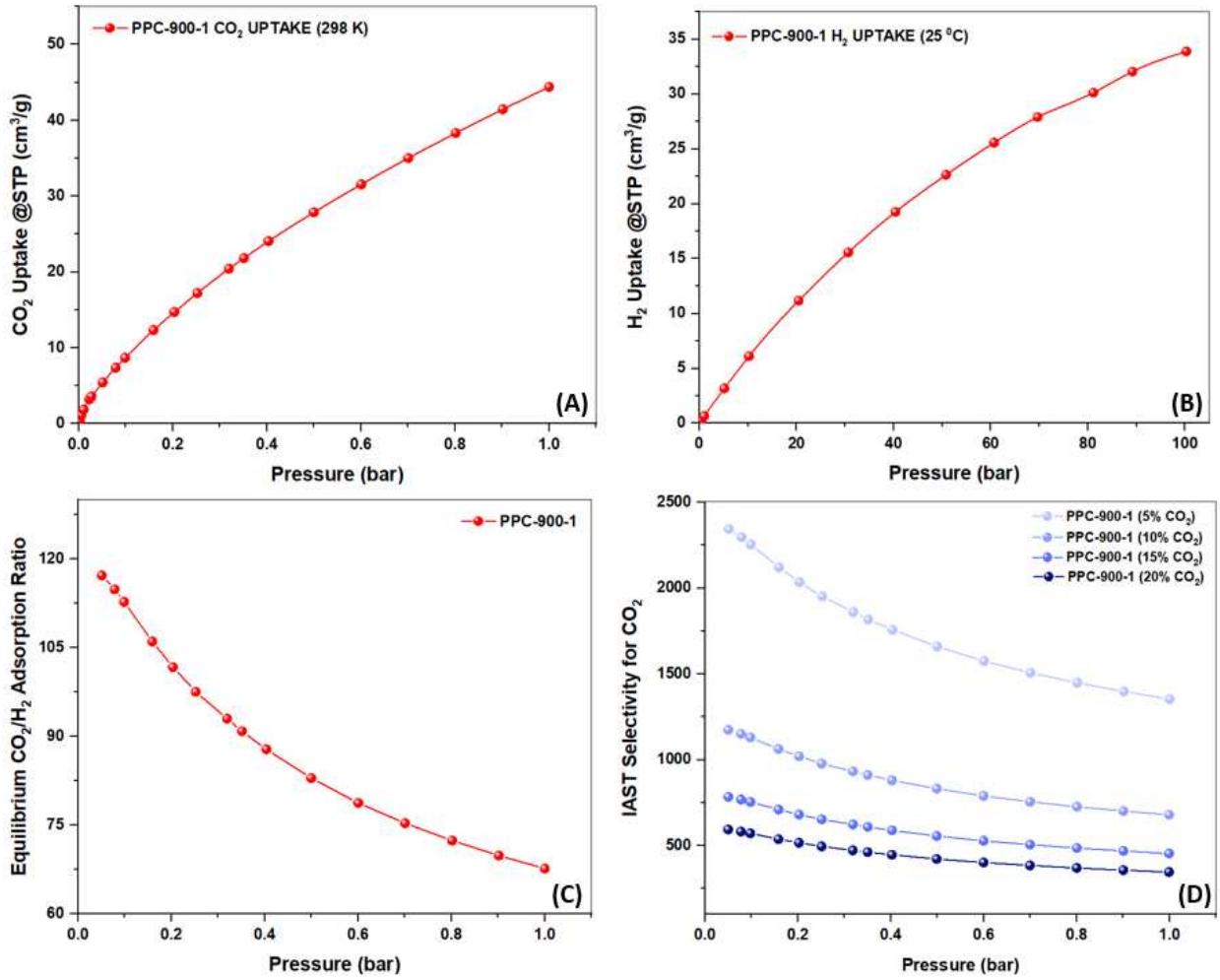


Fig. 9. (A) CO_2 Uptake isotherm at room temperature for synthesized PPC-900-1. (B) H_2 Uptake isotherm at room temperature for synthesized PPC-900-1. (C) CO_2/H_2 adsorption ratio equilibrium at 25 °C. (D) IAST Selectivity at 5-20% CO_2/H_2 mixture at 25 °C for PPC-900-1.

3.4. Techno-economic Results

Fig 10. illustrates the breakdown of sorbent production costs, highlighting the contributions of chemicals, utilities, and energy consumption. Among the chemicals, cyanuric acid was the most expensive ($16.6/kg), followed by methanol ($13.81/kg), DCE ($11.49/kg), benzene ($1.26/kg), and KOH ($0.89/kg), while $AlCl_3$ ($1.6/kg) and HCl ($0.27/kg) were relatively inexpensive.

For utilities, nitrogen represented the highest cost at $778.96/kg, followed by deionized water ($322.53/kg) and oil bath ($225.6/kg). Energy costs were dominated by heating ($65.62/kg), with

filtration and washing contributed to $23/kg, and drying incurring minimal expenses ($0.4/kg). Overall, utilities were identified as the dominant cost driver ($1327/kg), far exceeding energy ($89/kg) and chemical inputs ($45.92/kg). This distribution underscores the importance of utilities - particularly nitrogen and deionized water - in sorbent manufacturing. Heating was the most energy-intensive process, suggesting opportunities for cost reduction through improved efficiency or alternative technologies.

Fig. 11 examines the effect of operating conditions on chemical, energy, utility, and total costs, expressed both per kilogram and per unit area. This analysis is essential for identifying conditions that minimize operating expenses. As shown in Fig. 11, costs generally decrease with higher KOH ratios, reaching their lowest near a ratio of 4. Material synthesized at operating temperature of 600 °C with KOH ratio of 4, chemical costs dropped to $41.92/kg as shown in Fig. 11a, utilities to $675.9/kg as shown in Fig. 11b, and energy costs to $49.45/kg as shown in Fig. 11c, resulting in a total cost of $766.92/kg as shown in Fig. 11d. However, the total cost per area peaked at $2.15/m² as shown in Fig. 11e, indicating that this condition was not optimal.

At 900 °C and a KOH ratio of 1, heating requirements increased, raising energy costs to $89.03/kg. Nevertheless, the total cost per area fell to $0.74/m² as shown in Fig. 11e, the lowest recorded value. These results suggest that the optimum operating condition is at 900 °C and ratio 1. Overall, temperature strongly influences synthesis costs: higher temperatures generally increase expenses per kilogram, while offering advantages in cost per area and material performance. Thus, optimization requires balancing trade-offs between temperature and KOH ratio. From a quantitative perspective, lower-temperature processes are more economical per kilogram, but qualitatively, synthesis at 900 °C provides superior performance and cost efficiency per area.

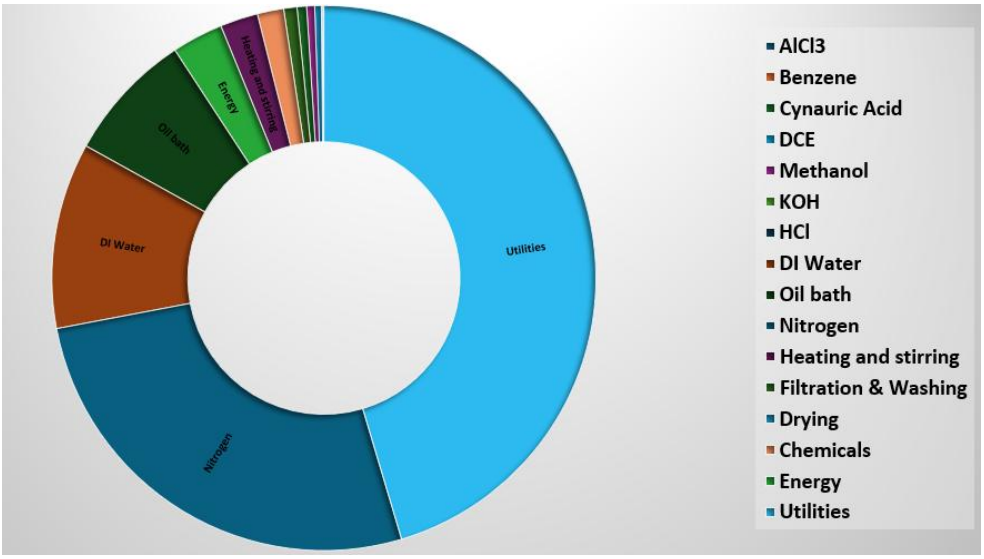


Fig. 10. Sorbent synthesis total cost breakdown of porous carbon material PPC-900-1.

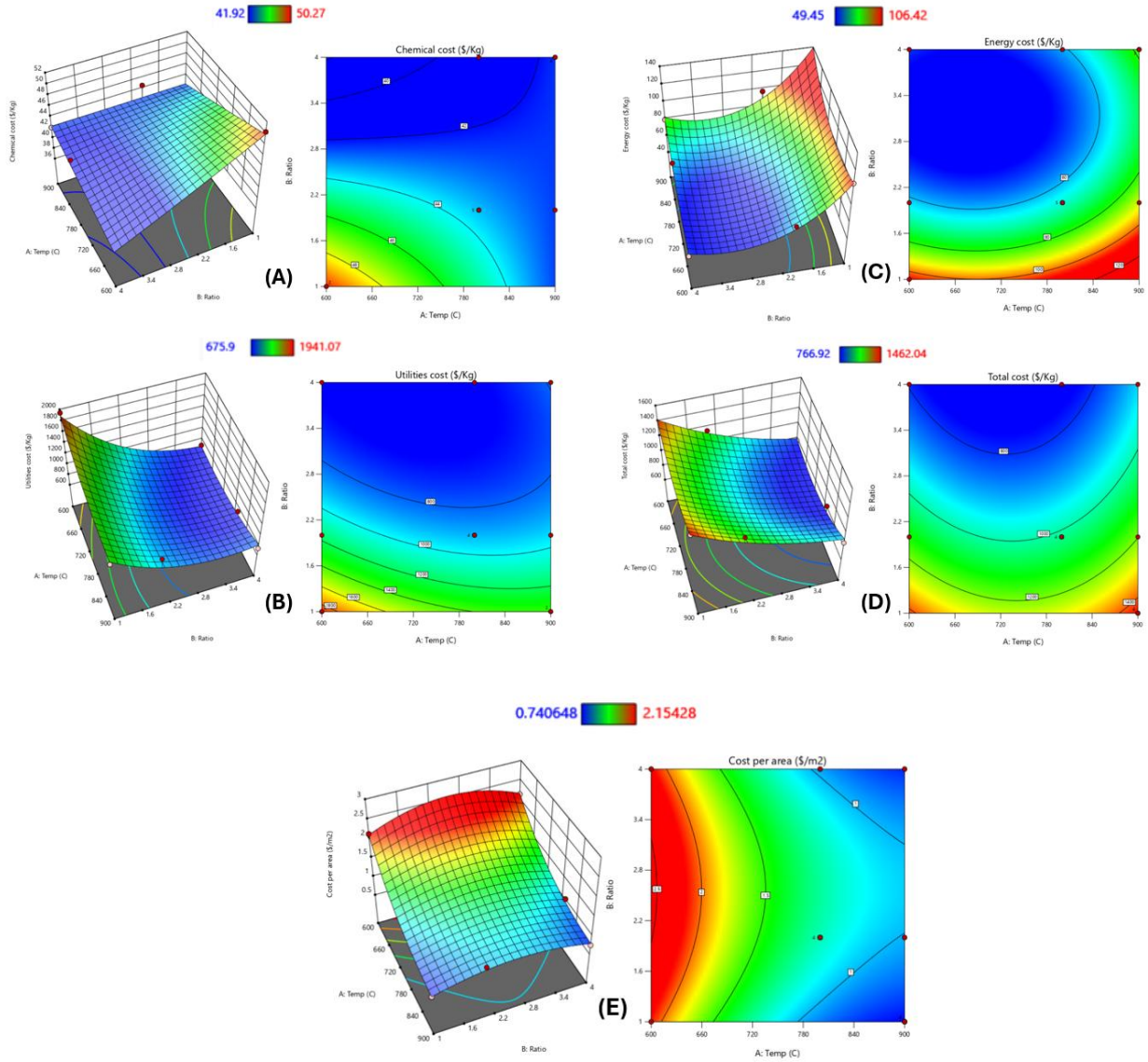


Fig. 11. Effect of PPC-900-1 Synthesis Conditions on; (A) chemical cost, (B) utilities cost, (C) energy cost, (D) total cost and (E) total cost/area.

4. Conclusion

This work demonstrates the successful development of a novel optimized micro–mesoporous carbon material, synthesized at temperature 900 °C and ratio 1:1 (PPC-900-1), exhibited 1969 m^2/g of high surface area and exceptionally 1.331 cm^3/g of pore volume, with its textural properties effectively tunable through controlled adjustment of activation temperature and activating agent dosage. These features enable strong CO_2 adsorption which comply with conditions of pre-combustion carbon capture. PPC-900-1 shows a favorable Qst at zero CO_2 loading of 17.8 kJ mol^{-1}, showing strong CO_2-sorbent interactions and high CO_2 uptake of 44 cm^3/g at low pressures. Most notably, PPC-900-1 exhibits excellent CO_2/H_2 selectivity of 2344 in a 5% CO_2/H_2 gas mixture. Collectively, these results highlight PPC-900-1 as a promising and efficient sorbent for CO_2 capture and hydrogen purification in future pre-combustion technologies.

Techno-economic study highlights the pivotal role of cost analysis in evaluating the economic feasibility of sorbent materials for carbon capture applications. A detailed breakdown revealed that utilities, particularly nitrogen and deionized water, represent the dominant contributors to overall production costs, far exceeding chemical and energy inputs. Energy consumption was largely driven by heating, underscoring the need for more efficient thermal processes.

The effect of operating conditions was further examined, showing that both temperature and KOH ratio significantly affect cost distribution. While lower temperatures and higher KOH ratios reduced costs per kilogram. The optimized porous carbon PPC-900-1 achieved the lowest cost per area and superior material performance. These findings emphasize the importance of balancing quantitative cost efficiency with qualitative material properties when determining optimal synthesis conditions. Future efforts should focus on reducing utility expenses and improving energy efficiency, thereby advancing the scalability of sorbent-based carbon capture technologies.

Acknowledgements
The authors acknowledge King Fahd University of Petroleum and Minerals, for providing the facilities and Cairo University for supporting this work.

Declaration of Interest Statement

The authors declare that they have no competing interests.

Data Availability

The datasets supporting the conclusions of this article are included within the article.

Funding

Funding was obtained from Cairo University.

Author information

Authors and Affiliations

Chemical Engineering Department, Faculty of Engineering, Cairo University, Giza 12613, Egypt
Process Technology Division, Engineering for the Petroleum and Process Industries (ENPPI), Cairo 11768, Egypt
Marwa A. El Maghraby

Interdisciplinary Research Center for Hydrogen Technologies and Carbon Management (IRC-HTCM), King Fahd University of Petroleum & Minerals, Dhahran 31261, Saudi Arabia
Mahmoud M. Abdelnaby

Chemical Engineering Department, Faculty of Engineering, Cairo University, Giza 12613, Egypt
School of Energy and Environmental Engineering, Nile University, Giza 12588, Egypt
Smart Engineering Systems Research Center (SESC), Nile University, Giza 12588, Egypt
A. O. Ghallab

Chemical Engineering Department, Faculty of Engineering, Cairo University, Giza 12613, Egypt
Nabil M. Abdelmonem

Authors' contributions

MA wrote up the main manuscript, conducted the results/analysis and prepared the figures. NA, AO and MM supervised the results, edited, read, and approved the final manuscript. The authors read and approved the final manuscript.

Authors' information

Prof. Dr. Nabil Mahmoud Abdel Monem is currently a professor of Chemical Engineering Department at Faculty of Engineering, Cairo University. Prof. Dr. Ayat Osama Ghallab is currently a professor of Chemical Engineering Department at Faculty of Engineering, Cairo University. Prof. Dr. Mahmoud Mohamed Abdelnaby is currently an assistant professor of Interdisciplinary Research Center for Hydrogen Technologies and Carbon Management (IRC-HTCM), King Fahd

University of Petroleum & Minerals. Eng. Marwa Ahmed El Maghraby is currently a principal process engineer at ENPPI (Engineering for Petroleum and Process Industries Company).

References

Abdalla, M. A., Zentou, H., Abdulhamid, M. A., Mohammed, M. G., Abdelnaby, M. M., & Abdelaziz, O. Y. (2025). A porous phenolic resin sorbent for enhanced CO2 capture: Synthesis, optimization, and techno-economic analysis. *Fuel*, *379*. https://doi.org/10.1016/j.fuel.2024.132961

Abdelnaby, M. M., Aliyu, M., Nemitallah, M. A., Alloush, A. M., Mahmoud, E. H. M., Ossoss, K. M., Zeama, M., & Dowaidar, M. (2023). Design and Synthesis of N-Doped Porous Carbons for the Selective Carbon Dioxide Capture under Humid Flue Gas Conditions. *Polymers*, *15*(11). https://doi.org/10.3390/polym15112475

Adeniji, A., Beda, A., Fioux, P., & Matei Ghimbeu, C. (2025). Engineering nitrogen-doped porous carbon positive electrodes for high-performance sodium-ion capacitors: the critical role of porosity, structure and surface functionalities. *Journal of Materials Chemistry A*, *13*(20), 14896–14914. https://doi.org/10.1039/D5TA01075F

Alabadi, A., Abbood, H. A., Li, Q., Jing, N., & Tan, B. (2016). Imine-Linked Polymer Based Nitrogen-Doped Porous Activated Carbon for Efficient and Selective CO2 Capture. *Scientific Reports*, *6*(1), 38614. https://doi.org/10.1038/srep38614

Alakbari, F. S., Mohyaldinn, M. E., Ayoub, M. A., Muhsan, A. S., Abdulkadir, S. J., Hussein, I. A., & Salih, A. A. (2023). Prediction of critical total drawdown in sand production from gas wells: Machine learning approach. *Canadian Journal of Chemical Engineering*, *101*(5), 2493–2509. https://doi.org/10.1002/cjce.24640

Avelar Dutra, F. V., Pires, B. C., Nascimento, T. A., Mano, V., & Borges, K. B. (2017). Polyaniline-deposited cellulose fiber composite prepared via in situ polymerization: enhancing adsorption properties for removal of meloxicam from aqueous media. *RSC Advances*, *7*(21), 12639–12649. https://doi.org/10.1039/C6RA27019K

Baliga, U. B. (2024, April 29). *The Role of Carbon Capture and Hydrogen in the Energy Transition*. https://doi.org/10.4043/35414-ms

Bandosz, T. J. (2021). *Porous Carbons as Oxygen Reduction Electrocatalysts* (pp. 41–77). https://doi.org/10.1007/978-3-030-65991-2_2

Boretti, A. (2025). Geological hydrogen storage: Current status, research frontiers, and the path to large-scale deployment. In *International Journal of Hydrogen Energy* (Vol. 134, pp. 54–63). Elsevier Ltd. https://doi.org/10.1016/j.ijhydene.2025.04.514

Caldwell, S. J., Al-Duri, B., Sun, N., Sun, C., Snape, C. E., Li, K., & Wood, J. (2015). Carbon Dioxide Separation from Nitrogen/Hydrogen Mixtures over Activated Carbon Beads: Adsorption Isotherms and Breakthrough Studies. *Energy & Fuels*, *29*(6), 3796–3807. https://doi.org/10.1021/acs.energyfuels.5b00164

Chen, J., Jiang, L., Wang, W., Shen, Z., Liu, S., Li, X., & Wang, Y. (2022). Constructing highly porous carbon materials from porous organic polymers for superior CO2 adsorption and separation. *Journal of Colloid and Interface Science*, *609*, 775–784. https://doi.org/10.1016/j.jcis.2021.11.091

Chen, X., Yang, J., Zhou, K., Lei, Z., Zhao, X., Zhang, J., & Luo, H. (2024). Preparation of Fe-doped hypercrosslinked poly(naphthalene-based) microporous carbon and its electrochemical properties. *Electrochimica Acta*, *491*. https://doi.org/10.1016/j.electacta.2024.144338

Choi, Y., Kim, K.-W., Park, B. J., Kim, T. Y., Lee, Y., Park, B., Kim, J. K., & Han, J. W. (2025). Rational design of nitrogen-doped porous carbon support on single atom catalysts for efficient CO_2 electroreduction. *Journal of Materials Chemistry A*, *13*(7), 4861–4869. https://doi.org/10.1039/D4TA08536A

Cong, H., Zhang, M., Chen, Y., Chen, K., Hao, Y., Zhao, Y., & Feng, L. (2015). Highly selective CO2 capture by nitrogen enriched porous carbons. *Carbon*, *92*, 297–304. https://doi.org/10.1016/j.carbon.2015.04.052

Cox, M., & Mokaya, R. (2017). Ultra-high surface area mesoporous carbons for colossal pre combustion CO_2 capture and storage as materials for hydrogen purification. *Sustainable Energy & Fuels*, *1*(6), 1414–1424. https://doi.org/10.1039/C7SE00300E

Deng, S., Wei, H., Chen, T., Wang, B., Huang, J., & Yu, G. (2014). Superior CO2 adsorption on pine nut shell-derived activated carbons and the effective micropores at different temperatures. *Chemical Engineering Journal*, *253*, 46–54. https://doi.org/10.1016/j.cej.2014.04.115

Du, Z., Nie, X., Deng, S., Zhao, L., Li, S., Zhang, Y., & Zhao, J. (2020). Comparative analysis of calculation method of adsorption isosteric heat: Case study of CO2 capture using MOFs. *Microporous and Mesoporous Materials*, *298*, 110053. https://doi.org/10.1016/j.micromeso.2020.110053

Echemi. (2025). *https://www.echemi.com/*.

El Maghraby, M. A., Essalhi, M., Zentou, H., Abdelmonem, N. M., Al-Yaseri, A. Z., & Abdelnaby, M. M. (2026). A porous carbon derived from hyper-crosslinked polymer for hydrogen Storage: Synthesis, characterization, techno-economic analysis. *International Journal of Hydrogen Energy*, *225*, 154480. https://doi.org/10.1016/j.ijhydene.2026.154480

Fan, X., Zhang, L., Zhang, G., Shu, Z., & Shi, J. (2013). Chitosan derived nitrogen-doped microporous carbons for high performance CO2 capture. *Carbon*, *61*, 423–430. https://doi.org/10.1016/j.carbon.2013.05.026

He, J., Gan, X., He, X., Zhang, K., & Cui, Y. (2025). Constructing hierarchical Si/PPy/PANI anodes with dual carbon layers for enhanced cycling stability and rate capability. *New Journal of Chemistry*. https://doi.org/10.1039/D5NJ02034D

Hryniewicka, A., Breczko, J., Siemiaszko, G., Markiewicz, K. H., Gabryelczyk, A., Lota, G., & Plonska-Brzezinska, M. E. (2025). Polymer-derived N-doped carbon nanomaterials containing carbon nano-onions and their potential applicability. *Materials Advances*, *6*(9), 2899–2910. https://doi.org/10.1039/d4ma01230e

Hu, T., Song, Y., Zhang, X., Lin, S., Liu, P., Zheng, C., & Gao, X. (2025). A mini review for hydrogen production routes toward carbon neutrality. *Propulsion and Energy*, *1*(1). https://doi.org/10.1007/s44270-024-00004-4

Hui, B., Zhou, H., Liu, A., Fei, C., Xu, T., Chen, C., Ju, D., Ma, H., Zhu, Z., & Mao, R. (2025). Nitrogen-rich self-doping modified porous carbon material as a CDI electrode for brine desalination. *Carbon Letters*, *35*(4), 1701–1714. https://doi.org/10.1007/s42823-025-00891-w

Imarcgroup. (2025). *https://www.imarcgroup.com/nitrogen-pricing-report*.

Jadhav, P., & Joshi, G. M. (2021). Recent trends in Nitrogen doped polymer composites: a review. In *Journal of Polymer Research* (Vol. 28, Number 3). Springer Science and Business Media B.V. https://doi.org/10.1007/s10965-021-02436-x

Jankovic, J., & Wilkinson, D. P. (2025). Towards a more sustainable future: Transitioning from thermochemical to electrochemical processes in clean energy technologies relevant to hydrogen-containing fuels. *Canadian Journal of Chemical Engineering*, *103*(4), 1602–1622. https://doi.org/10.1002/cjce.25549

Jimenez-Lopez, L., Morales Ospino, R., de Araujo, L. G., Celzard, A., & Fierro, V. (2025). Latest developments in the synthesis of metal-organic frameworks and their hybrids for hydrogen storage. In *Nanoscale*. Royal Society of Chemistry. https://doi.org/10.1039/d4nr03969f

Keskin, S., van Heest, T. M., & Sholl, D. S. (2010). Can Metal–Organic Framework Materials Play a Useful Role in Large-Scale Carbon Dioxide Separations? *ChemSusChem*, *3*(8), 879–891. https://doi.org/10.1002/cssc.201000114

Khosrowshahi, M. S., Mashhadimoslem, H., Shayesteh, H., Singh, G., Khakpour, E., Guan, X., Rahimi, M., Maleki, F., Kumar, P., & Vinu, A. (2023). Natural Products Derived Porous Carbons for CO2 Capture. In *Advanced Science* (Vol. 10, Number 36). John Wiley and Sons Inc. https://doi.org/10.1002/advs.202304289

Kim, K. H., & Kim, M. H. (2023). Adsorption of CO2, CO, H2, and N2 on Zeolites, Activated Carbons, and Metal-Organic Frameworks with Different Surface Nonuniformities. *Sustainability (Switzerland)*, *15*(15). https://doi.org/10.3390/su151511574

Kunjumon, J., Maria Ruban, A., Kaur, H., Sajan, D., Mahasivam, S., Bansal, V., Singh, G., & Vinu, A. (2025a). Functionalized Nanoporous Biocarbon with High Specific Surface Area Derived from Waste Hardwood Chips for CO2 Capture and Supercapacitors. *Small Science*. https://doi.org/10.1002/smsc.202500174

Kunjumon, J., Maria Ruban, A., Kaur, H., Sajan, D., Mahasivam, S., Bansal, V., Singh, G., & Vinu, A. (2025b). Functionalized Nanoporous Biocarbon with High Specific Surface Area Derived from Waste Hardwood Chips for CO2 Capture and Supercapacitors. *Small Science*. https://doi.org/10.1002/smsc.202500174

Lee, Y. J., Talapaneni, S. N., & Coskun, A. (2017). Chemically Activated Covalent Triazine Frameworks with Enhanced Textural Properties for High Capacity Gas Storage. *ACS Applied Materials & Interfaces*, *9*(36), 30679–30685. https://doi.org/10.1021/acsami.7b08930

Li, Y., Ben, T., Zhang, B., Fu, Y., & Qiu, S. (2013). Ultrahigh gas storage both at low and high pressures in KOH-activated carbonized porous aromatic frameworks. *Scientific Reports*, *3*. https://doi.org/10.1038/srep02420

Li, Y., Zou, B., Hu, C., & Cao, M. (2016). Nitrogen-doped porous carbon nanofiber webs for efficient CO2 capture and conversion. *Carbon*, *99*, 79–89. https://doi.org/10.1016/j.carbon.2015.11.074

Liang, Z., Liu, H., Zeng, J., Zhou, J., Li, H., & Xia, H. (2018). Facile Synthesis of Nitrogen-Doped Microporous Carbon Spheres for High Performance Symmetric Supercapacitors. *Nanoscale Research Letters*, *13*. https://doi.org/10.1186/s11671-018-2713-0

Liu, H., Shin, H., Li, X. Y., Su, G., Ou, P., Wang, Y., Chen, L., Yu, J., Chen, Y., Xia, R., Lee, G., Lee, K. S., Yu, C., Wang, P., Choi, D., Zhou, D., Tian, C., Gereige, I., Alahmed, A., … Sargent, E. H. (2025). Hierarchically porous carbon supports enable efficient syngas production in electrified reactive capture. *Energy and Environmental Science*. https://doi.org/10.1039/d5ee00094g

Ma, C., Min, J., Gong, J., Liu, X., Mu, X., Chen, X., & Tang, T. (2020). Transforming polystyrene waste into 3D hierarchically porous carbon for high-performance supercapacitors. *Chemosphere*, *253*. https://doi.org/10.1016/j.chemosphere.2020.126755

Ma, C., Xu, X., Xu, M., Zhou, Y., Yao, Y., Xiang, Z., He, W., Yu, J., Zhang, Q., Feng, F., Liu, Y., Yin, C., Li, X., & Lu, C. (2025). NCQD-induced nitrogen configuration engineering for constructing hybrid CN with exceptionally high nitrogen content and predominantly pyrrolic/pyridinic-N for catalytic hydrogenation. *Journal of Materials Chemistry A*, *13*(17), 12507–12522. https://doi.org/10.1039/D4TA08732A

Mahurin, S. M., Górka, J., Nelson, K. M., Mayes, R. T., & Dai, S. (2014). Enhanced CO2/N2 selectivity in amidoxime-modified porous carbon. *Carbon*, *67*, 457–464. https://doi.org/10.1016/j.carbon.2013.10.018

Maka, A. O. M., & Mehmood, M. (2024). Green hydrogen energy production: current status and potential. In *Clean Energy* (Vol. 8, Number 2, pp. 1–7). Oxford University Press. https://doi.org/10.1093/ce/zkae012

Makaryan, I. A., & Sedov, I. V. (2023). Progress of Commercial Technologies for Producing Syngas and Hydrogen from Hydrocarbon Gases. *Russian Journal of Applied Chemistry*, *96*(6), 619–642. https://doi.org/10.1134/S1070427223060010

Maniarasu, R., Rathore, S. K., & Murugan, S. (2023). Biomass-based activated carbon for CO_2 adsorption–A review. *Energy & Environment*, *34*(5), 1674–1721. https://doi.org/10.1177/0958305X221093465

Maniarasu, R, Rathore, Sushil Kumar, & Murugan, S. (2021). A review on materials and processes for carbon dioxide separation and capture. *Energy & Environment*, *34*(1), 3–57. https://doi.org/10.1177/0958305X211050984

Marafiq Saudi Arabia. (2025). *https://marafiq.com.sa/en/partnering-with-us/water-tariff/*.

Mekonnin, A. S., Wacławiak, K., Humayun, M., Zhang, S., & Ullah, H. (2025). Hydrogen Storage Technology, and Its Challenges: A Review. In *Catalysts* (Vol. 15, Number 3). Multidisciplinary Digital Publishing Institute (MDPI). https://doi.org/10.3390/catal15030260

Min, H., Zhang, K., Guo, Z., Chi, F., Fu, L., Li, B., Qiao, X., Wang, S., Cao, S., Wang, B., & Ma, Q. (2023). N-rich chitosan-derived porous carbon materials for efficient CO2 adsorption and gas separation. *Frontiers in Chemistry*, *11*. https://doi.org/10.3389/fchem.2023.1333475

Mishra, S., Pradhan, L., & Jena, B. K. (2025). Review on Carbon Nanostructures for Supercapacitors: Cutting-Edge Energy Storage Applications and Perspectives. *Energy & Fuels*, *39*(28), 13151–13182. https://doi.org/10.1021/acs.energyfuels.5c01207

Mollahosseini, A., Nikkhah Dafchahi, M., Khoshhal Salestan, S., Chew, J. W., Mozafari, M., Soroush, M., Hrapovic, S., Hemraz, U. D., Giro, R., Steiner, M. B., La, Y. H., Seyedpour Taji, S. F., Azyat, K., Islam, M. A., Kavyani, S., Wang, X., Cho, J. Y., & Sadrzadeh, M. (2025). Polymeric membranes in carbon capture, utilization, and storage: current trends and future directions in decarbonization of industrial flue gas and climate change mitigation. In *Energy and Environmental Science* (Vol. 18, Number 11, pp. 5025–5092). Royal Society of Chemistry. https://doi.org/10.1039/d4ee05328a

Morales-Ospino, R., Reinert, L., Izquierdo, M. T., Celzard, A., Duclaux, L., & Fierro, V. (2025). Challenges and insights in CO2 adsorption using N-doped carbons under realistic conditions. *Environmental Research*, *273*. https://doi.org/10.1016/j.envres.2025.121211

Nuhnen, A., & Janiak, C. (2020). A practical guide to calculate the isosteric heat/enthalpy of adsorption *via* adsorption isotherms in metal–organic frameworks, MOFs. *Dalton Transactions*, *49*(30), 10295–10307. https://doi.org/10.1039/D0DT01784A

Park, Y., Moon, D. K., Kim, Y. H., Ahn, H., & Lee, C. H. (2014). Adsorption isotherms of CO2, CO, N2, CH4, Ar and H2 on activated carbon and zeolite LiX up to 1.0 MPa. *Adsorption*, *20*(4), 631–647. https://doi.org/10.1007/s10450-014-9608-x

Peter, S. E., Thomas, P., Vairavel, P., & Anil Kumar, N. V. (2024). Cyanuric chloride as a linker towards the synthesis of covalent triazine polymers: a review. In *Materials Advances* (Vol. 5, Number 23, pp. 9175–9209). Royal Society of Chemistry. https://doi.org/10.1039/d4ma00739e

Pinto, P. S., Silva, R. C. F., de Freitas Filho, R. L., Santos, L. O., Pereira, S. D., & Teixeira, A. P. C. (2025). Mesoporous Carbon-Based Materials Obtained from Biomass and Their Application in the Adsorption of Contaminants: A Review. In *Journal of the Brazilian Chemical Society* (Vol. 36, Number 7). Sociedade Brasileira de Quimica. https://doi.org/10.21577/0103-5053.20250068

Rana, A., & Andino, J. M. (2025). A Review of Materials for Carbon Dioxide Capture. In *Catalysts* (Vol. 15, Number 3). Multidisciplinary Digital Publishing Institute (MDPI). https://doi.org/10.3390/catal15030273

Saudi Electricity Global Petrol. (2025). *https://www.globalpetrolprices.com/Saudi-Arabia/electricity_prices/*.

Segovia-Hernández, J. G., Hernández, S., Cossío-Vargas, E., Juarez-García, M., & Sánchez-Ramírez, E. (2024). Green hydrogen production for sustainable development: a critical examination of barriers and strategic opportunities. In *RSC Sustainability*. Royal Society of Chemistry. https://doi.org/10.1039/d4su00630e

Sethia, G., & Sayari, A. (2015). Comprehensive study of ultra-microporous nitrogen-doped activated carbon for CO2 capture. *Carbon*, *93*, 68–80. https://doi.org/10.1016/j.carbon.2015.05.017

Sevilla, M., Valle-Vigón, P., & Fuertes, A. B. (2011). N-Doped Polypyrrole-Based Porous Carbons for CO_2 Capture. *Advanced Functional Materials*, *21*(14), 2781–2787. https://doi.org/10.1002/adfm.201100291

Shang, Y., Ding, Y., Zhang, P., Wang, M., Jia, Y., Xu, Y., Li, Y., Fan, K., & Sun, L. (2022). Pyrrolic N or pyridinic N: The active center of N-doped carbon for CO2 reduction. *Chinese Journal of Catalysis*, *43*(9), 2405–2413. https://doi.org/10.1016/S1872-2067(22)64122-6

Streb, A., Hefti, M., Gazzani, M., & Mazzotti, M. (2019). Novel Adsorption Process for Co-Production of Hydrogen and CO2 from a Multicomponent Stream. *Industrial & Engineering Chemistry Research*, *58*(37), 17489–17506. https://doi.org/10.1021/acs.iecr.9b02817

Sumida, K., Rogow, D. L., Mason, J. A., McDonald, T. M., Bloch, E. D., Herm, Z. R., Bae, T.-H., & Long, J. R. (2012). Carbon Dioxide Capture in Metal–Organic Frameworks. *Chemical Reviews*, *112*(2), 724–781. https://doi.org/10.1021/cr2003272

Sun, L., Tian, C., Fu, Y., Yang, Y., Yin, J., Wang, L., & Fu, H. (2014). Nitrogen-Doped Porous Graphitic Carbon as an Excellent Electrode Material for Advanced Supercapacitors. *Chemistry – A European Journal*, *20*(2), 564–574. https://doi.org/10.1002/chem.201303345

Sun, Y.-B., Cao, C.-Y., Yang, S.-L., Huang, P.-P., Wang, C.-R., & Song, W.-G. (2014). C_{60} fullerenol as an active and stable catalyst for the synthesis of cyclic carbonates from CO_2 and epoxides. *Chem. Commun.*, *50*(71), 10307–10310. https://doi.org/10.1039/C4CC04891A

Suo, X., Xia, L., Yang, Q., Zhang, Z., Bao, Z., Ren, Q., Yang, Y., & Xing, H. (2017). Synthesis of anion-functionalized mesoporous poly(ionic liquid)s via a microphase separation-hypercrosslinking strategy: highly efficient adsorbents for bioactive molecules. *Journal of Materials Chemistry A*, *5*(27), 14114–14123. https://doi.org/10.1039/C7TA01986F

Tachibana, N., Kanai, M., Kamezaki, Y., & Somekawa, S. (2022). Enhanced nitrogen doping in porous carbon and its composite with MnO2 as an efficient oxygen reduction catalyst for Mg–air batteries. *Journal of Materials Science*, *57*(33), 15929–15942. https://doi.org/10.1007/s10853-022-07639-1

Taşğın, B., Ryšavý, J., Sangeetha, T., & Yan, W.-M. (2025). Hydrogen Storage in Zeolites: A Mini Review of Structural and Chemical Influences on Adsorption Performance. *Green Energy and Fuel Research*. https://doi.org/10.53941/gefr.2025.100005

Thommes, M., Kaneko, K., Neimark, A. V, Olivier, J. P., Rodriguez-Reinoso, F., Rouquerol, J., & Sing, K. S. W. (2015). *Physisorption of gases, with special reference to the evaluation of surface area and pore size distribution (IUPAC Technical Report)*. *Pure and Applied Chemistry*, *87*(9–10), 1051–1069. https://doi.org/doi:10.1515/pac-2014-1117

Tian, L., Zhi, Y., Yu, Q., Xu, Q., Demir, M., Colak, S. G., Farghaly, A. A., Wang, L., & Hu, X. (2024). Enhanced CO2 Adsorption Capacity in Highly Porous Carbon Materials Derived from Melamine-Formaldehyde Resin. *Energy & Fuels*, *38*(14), 13186–13195. https://doi.org/10.1021/acs.energyfuels.4c02372

van der Spek, M., Banet, C., Bauer, C., Gabrielli, P., Goldthorpe, W., Mazzotti, M., Munkejord, S. T., Røkke, N. A., Shah, N., Sunny, N., Sutter, D., Trusler, J. M., & Gazzani, M. (2022). Perspective on the hydrogen economy as a pathway to reach net-zero CO2 emissions in Europe†. *Energy and Environmental Science*, *15*(3), 1034–1077. https://doi.org/10.1039/d1ee02118d

Van Der Voort, P., Ravikovitch, P. I., De Jong, K. P., Benjelloun, M., Van Bavel, E., Janssen, A. H., Neimark, A. V, Weckhuysen, B. M., & Vansant, E. F. (2002). A New Templated Ordered Structure with Combined Micro- and Mesopores and Internal Silica Nanocapsules. *The Journal of Physical Chemistry B*, *106*(23), 5873–5877. https://doi.org/10.1021/jp025642i

Vanreppelen, K., Schreurs, S., Kuppens, T., Thewys, T., Carleer, R., & Yperman, J. (2013). Activated carbon by co-pyrolysis and steam activation from particle board and melamine formaldehyde resin: Production, adsorption properties and techno economic evaluation. *Journal of Sustainable Development of Energy, Water and Environment Systems*, *1*(1), 41–57. https://doi.org/10.13044/j.sdewes.2013.01.0004

Vogt, E. T. C., & Weckhuysen, B. M. (2024). The refinery of the future. *Nature*, *629*(8011), 295–306. https://doi.org/10.1038/s41586-024-07322-2

Vorokhta, M., Kusdhany, M. I. M., Švábová, M., Nishihara, M., Sasaki, K., & Lyth, S. M. (2025). Hierarchically porous carbon foams coated with carbon nitride: Insights into adsorbents for pre-combustion and post-combustion CO2 separation. *Separation and Purification Technology*, *354*. https://doi.org/10.1016/j.seppur.2024.129054

Wabo, S. G., & Klepel, O. (2021). Nitrogen release and pore formation through KOH activation of nitrogen-doped carbon materials: an evaluation of the literature. *Carbon Letters*, *31*(4), 581–592. https://doi.org/10.1007/s42823-021-00252-3

Wang, J., Senkovska, I., Oschatz, M., Lohe, M. R., Borchardt, L., Heerwig, A., Liu, Q., & Kaskel, S. (2013). Highly porous nitrogen-doped polyimine-based carbons with adjustable microstructures for CO2 capture. *Journal of Materials Chemistry A*, *1*(36), 10951. https://doi.org/10.1039/c3ta11995e

Wang, K., Lin, G., Meng, J., Guo, J., Tan, B., Liu, S., Lin, Q., Wu, X., & Gao, X. (2024). Textural properties prediction of KOH-activated carbon prepared from coal based on pyrolysis kinetics. *Waste Disposal & Sustainable Energy*, *6*(4), 487–500. https://doi.org/10.1007/s42768-024-00204-3

Warrag, & See. (n.d.). *Capturing impurities from oil and gas using deep eutectic solvents Citation for*. Retrieved www.tue.nl/taverne

Wilkes, M. D. (2023). *Techno-Economic Analysis of CO 2 Capture Technologies for Small-Scale Dispatchable Gas Turbines*.

Xing, W., Liu, C., Zhou, Z., Zhang, L., Zhou, J., Zhuo, S., Yan, Z., Gao, H., Wang, G., & Qiao, S. Z. (2012). Superior CO2 uptake of N-doped activated carbon through hydrogen-bonding interaction. *Energy & Environmental Science*, *5*(6), 7323. https://doi.org/10.1039/c2ee21653a

Xu, C., Bacsik, Z., & Hedin, N. (2015). Adsorption of CO_2 on a micro-/mesoporous polyimine modified with tris(2-aminoethyl)amine. *Journal of Materials Chemistry A*, *3*(31), 16229–16234. https://doi.org/10.1039/C5TA01321F

Yang, X., Yu, M., Zhao, Y., Zhang, C., Wang, X., & Jiang, J. X. (2014). Remarkable gas adsorption by carbonized nitrogen-rich hypercrosslinked porous organic polymers. *Journal of Materials Chemistry A*, *2*(36), 15139–15145. https://doi.org/10.1039/c4ta02782e

Yu, Q., Bai, J., Huang, J., Demir, M., Farghaly, A. A., Aghamohammadi, P., Hu, X., & Wang, L. (2023). One-Pot Synthesis of Melamine Formaldehyde Resin-Derived N-Doped Porous Carbon for CO2 Capture Application. *Molecules*, *28*(4). https://doi.org/10.3390/molecules28041772

Zelenak, V., Halamova, D., Gaberova, L., Bloch, E., & Llewellyn, P. (2008). Amine-modified SBA-12 mesoporous silica for carbon dioxide capture: Effect of amine basicity on sorption properties. *Microporous and Mesoporous Materials*, *116*(1–3), 358–364. https://doi.org/10.1016/j.micromeso.2008.04.023

Zeng, H., Qu, X., Xu, D., & Luo, Y. (2022). Porous Adsorption Materials for Carbon Dioxide Capture in Industrial Flue Gas. *Frontiers in Chemistry*, *10*. https://doi.org/10.3389/fchem.2022.939701

Zeng, R., Jiang, H., Lai, N., Yang, H., Xu, Y., & Bai, W. (2021). Preparation and application of microporous carbons as excellent adsorbents for reversible iodine capture and efficient removal of dye. *Diamond and Related Materials*, *120*. https://doi.org/10.1016/j.diamond.2021.108718

Zhang, P., Zhong, Y., Ding, J., Wang, J., Xu, M., Deng, Q., Zeng, Z., & Deng, S. (2019). A new choice of polymer precursor for solvent-free method: Preparation of N-enriched porous carbons for highly selective CO2 capture. *Chemical Engineering Journal*, *355*, 963–973. https://doi.org/10.1016/j.cej.2018.08.219

Zhang, X., Peng, X., Liu, S., Liu, X., Liu, G., Liu, R., Niu, J., Yuan, Z., Zhang, J., Yi, X., & Filatov, S. (2025). Melamine-derived nitrogen-doped carbon foam supported bimetallic NiZn-MOFs as an efficient adsorbent for CH4 storage. *Journal of Porous Materials*, *32*(4), 1309–1319. https://doi.org/10.1007/s10934-025-01758-1

Zhigang Liu, Qiang Zhang, & Bingsen Zhang. (2025). *Carbon Catalysis*.

Zhou, J., Li, Z., Xing, W., Zhu, T., Shen, H., & Zhuo, S. (2015). N-doped microporous carbons derived from direct carbonization of K^+ exchanged *meta* -aminophenol–formaldehyde resin for superior CO_2 sorption. *Chemical Communications*, *51*(22), 4591–4594. https://doi.org/10.1039/C4CC10364E